Electronic Supplementary Material (ESI) for Physical Chemistry Chemical Physics.

Manipulating Stereoselectivity of Parahydrogen Addition to Acetylene to Unravel Interconversion of Ethylene Nuclear Spin Isomers

Sergey V. Sviyazov,[a,b] Simon V. Babenko,[a,c] Ivan V. Skovpin,[a] Larisa M. Kovtunova,[a,d] Nikita V. Chukanov,[a,b] Alexander Yu. Stakheev,[e] Dudari B. Burueva,*[a] and Igor V. Koptyug*[a]

[a] Laboratory of Magnetic Resonance Microimaging, International Tomography Center, SB RAS, Novosibirsk 630090, Russia
[b] Novosibirsk State University, Novosibirsk 630090, Russia
[c] V.V. Voevodsky Institute of Chemical Kinetics and Combustion, SB RAS, Novosibirsk 630090, Russia
[d] Boreskov Institute of Catalysis, SB RAS, Novosibirsk 630090, Russia
[e] N.D. Zelinsky Institute of Organic Chemistry, RAS, Moscow 119991, Russia

E-mails:
* burueva@tomo.nsc.ru, koptyug@tomo.nsc.ru

Table of Contents

Experimental Procedures

1.1. Materials

Acetylene (99.5%; PromGas, Russia) and hydrogen (> 99.999%; AlfaGas, Russia) gases were used without additional purification. Parahydrogen (p-H_2) at > 98% enrichment was generated by passing hydrogen gas over a hydrated iron oxide FeO(OH) catalyst (371254, Sigma-Aldrich) in a closed-cycle cryostat operating at 21 K (CryoPribor, Russia). Deuterated water (99.8 atom % D; Solvex, Russia) was used as a solvent. Liquid bromine Br_2 (99.3%) and 2-bromoethanol (95%; B65586, Sigma-Aldrich) were used as received.

Pd/TiO_2 catalyst was prepared by incipient-wetness impregnation of titania with an aqueous solution containing palladium (II) nitrate to obtain 1 wt% Pd metal loading. The detailed procedure of catalyst preparation is described elsewhere.[1] Immobilized Ir catalyst (denoted as Ir-P@SiO_2) was prepared via the interaction of [$Ir_2(COD)_2(\mu\text{-}Cl)_2$] dimeric complex (99%; 77-0400, STREM Chemicals) with -PPh_2 groups of 2-diphenylphosphinoethyl-functionalized silica (538019, Sigma-Aldrich); the details of catalyst preparation[2] and catalyst characterization[3] are described elsewhere. The Ir metal loading of ~4 wt.% was found by elemental analysis. The bimetallic Pd-In/γ-Al_2O_3 catalyst (1 wt.% Pd; the Pd : In molar ratio is 1 : 1) was characterized in recent publications.[4–6]

1.2. Ethylene production

Ethylene was produced via selective heterogeneous hydrogenation of acetylene. Acetylene and p-H_2 were premixed in the molar ratio of 1 : 4. The catalyst (20-30 mg) was placed in the middle of a stainless-steel tubular reactor (6.3 mm o.d., 4.2 mm i.d., 20 cm total length) between two plugs of fiberglass tissue. The bimetallic Pd-In catalyst was preliminarily reduced in H_2 flow at 400 °C for 1 h before each experiment to ensure the formation of the intermetallic Pd-In compound. It was then cooled down to the desired temperature without H_2 termination, and acetylene/p-H_2 mixture was introduced to the catalyst. Other catalysts (Ir-P@SiO_2 and Pd/TiO_2) were used without additional treatment. The reactor was positioned outside an NMR spectrometer and substrate gas mixture was supplied to the reactor; the reactor effluent was supplied through a PTFE capillary (0.79 mm i.d.) to a standard screw-cap 10 mm o.d. NMR tube (513-3PP-7; Wilmad) positioned inside the NMR spectrometer. In the NMR tube, the gas mixture was flowing from the bottom to the top and then to a vent through a PTFE tubing (1.59 mm i.d.) through a wye-type fitting. Conversion and selectivity to ethylene were evaluated for each catalyst from ^{1}H NMR spectra acquired at thermal equilibrium. The volumetric feed flow rates were regulated using a precalibrated rotameter (Aalborg Instruments & Controls). All experiments were performed at ambient pressure. The reactor was heated with a tubular furnace and temperature was controlled with a K-type thermocouple placed adjacent to the catalyst bed on the external side of the reactor.

1.3. Ethylene symmetry breaking reaction

Ethylene and Br_2 react in deuterated water to yield bromohydrin – 2-bromoethan(^{2}H)ol (further denoted as BrEtOD). A drop of Br_2 was placed at the bottom of an NMR tube containing D_2O to maintain a saturated bromine solution. Free bromine solution was titrated with sodium thiosulfate in the presence of potassium iodide using starch as an indicator. Five independent titrations were performed and the concentration was found to be 0.14±0.02 M. Such concentration ensured fast and complete reaction (in less than a second) with ethylene when the produced ethylene gas was bubbled through bromine water in a 10 mm NMR tube located in the NMR probe inside the magnet. For a control experiment, acetylene/p-H_2 mixture was flowing at 200 sccm flow rate to the reactor and the reactor effluent was bubbled for 10 s (unless stated otherwise) through bromine water using a PFTE capillary (0.79 mm i.d.) of minimal length to minimize the travel time. ^{1}H NMR spectra were then acquired. Hydrolysis of BrEtOD to ethan-1,2-di($^2H_2$)ol was negligible on the experimental timescale.

The experiment with a variable ethylene storage time was performed as follows: the reactor effluent was collected in a 60 mL syringe (made of polypropylene; with luer lock) at the rate of 3 mL/s. The storage time calculations are described in Section 3.4 below. The gas supply system to the NMR tube was equipped with several leak-tight PEEK valves (P-733, Idex Health & Science) to ensure an oxygen-free experiment.

1.4. NMR experiments

All PASADENA ^{1}H NMR experiments were performed on a 7.05 T AV 300 NMR instrument (Bruker). A 10 mm BBO 300 MHz Bruker probe head was used. For signal enhancement (*SE*) calculations, ^{1}H PASADENA NMR spectra were acquired using a π/4 rf pulse. ^{1}H NMR spectra of the reaction mixture at thermal equilibrium were acquired using a π/2 rf pulse. For NMR lineshape analysis and kinetics measurements we employed OPSYd-12 pulse sequence[7] in order to suppress the contributions of thermally polarized BrEtOD signals.

For scalar proton-proton couplings (*J*-couplings) elucidation, ^{1}H NMR spectra of 2-bromoethanol in distilled water (85 mM) were acquired on a 1.4 T SpinSolve Ultra system (Magritek). The ^{1}H-^{1}H *J*-coupling constants in BrEtOD are presented in Section 3.1 of this SI.

General Considerations

2.1. The origin of ethylene nuclear spin isomers in quantum mechanics

Ethylene ($^{12}C_2{}^1H_4$) is a symmetrical molecule with four equivalent protons. Ethylene molecule has three twofold symmetry axes, three symmetry planes, an inversion center, and, therefore, belongs to the D_{2h} molecular point group. In this work, we used the molecular reference frame shown in Fig. S1. The labeling of the reference frame axes affects only the designations of irreducible representations that describe the symmetry of the wave function, but this does not affect the properties of ethylene itself.

For polyatomic high-symmetry molecules, according to the Pauli principle upon the permutation of any pair of identical fermions the total wavefunction changes its sign. This is also often referred to as a consequence of the symmetrization postulate. The operations C_2^z, C_2^x, C_2^y result in a permutation of an even number of pairs of fermions meaning that the total wavefunction does not change (the total wavefunction sign changes an even number of times). Consequently, when transforming the total wave function, the characters for the operations C_2^z, C_2^x, C_2^y turn out to be equal to +1. This means that the complete wave function is characterized by a one-dimensional irreducible representation A. Next, we consider specifically the classification of rotational and nuclear wavefunctions according to the symmetry.

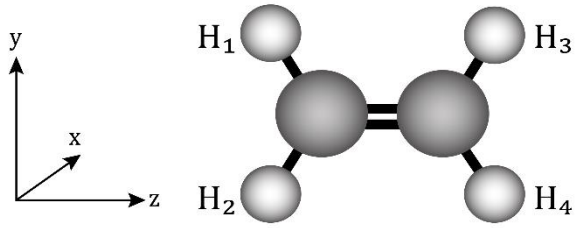

Figure S1. The reference frame and the numbering of protons in ethylene used in this work.

Each proton (spin ½) in ethylene molecule has two possible projections $|\alpha\rangle(+\frac{1}{2})$ or $|\beta\rangle$ $(-\frac{1}{2})$. Therefore, ethylene molecule is described by sixteen nuclear spin wavefunctions differing in the orientation of four spins. These sixteen wavefunctions form a representation for which one can find characters over all symmetry operations in the D_{2h} group. The reducible representation is decomposed into irreducible representations as follows[8]:

$$reducible\ representation\ = 7A_g + 3B_{1u} + 3B_{2u} + 3B_{3g}.$$

Consequently, sixteen nuclear spin wavefunctions are grouped according to four irreducible representations: A_g, B_{1u}, B_{2u}, and B_{3g} (the statistical ratio is 7 : 3 : 3 : 3). Also, nuclear spin wavefunctions can be classified according to the total nuclear spin *I*. The total spin of four spins ½ can be 2, 1, or 0. It is shown elsewhere[8] that seven wave functions characterized by A_g symmetry are divided into five functions with *I*=2, and two functions with *I*=0, whereas all wave functions characterized by B_{1u}, B_{2u}, B_{3g} symmetries have *I*=1.

It can also be shown that rotational wavefunctions are systematized according to four irreducible representations: A_g, B_{1g}, B_{2g}, and B_{3g}.[9] The total wavefunction has either A_g or A_u symmetry. We assume that ethylene molecule is in the ground vibrational and electronic state and, therefore, the vibrational and rotational wave functions are characterized by the A_g symmetry. Therefore, the following combinations of rotational and nuclear wave functions are allowed:

$$A_g = A_g^{nuc} \cdot A_g^{rot};$$

$$A_g = B_{3g}^{nuc} \cdot B_{3g}^{rot};$$

$$A_u = B_{1u}^{nuc} \cdot B_{1g}^{rot};$$

$$A_u = B_{2u}^{nuc} \cdot B_{2g}^{rot}.$$

These relations determine the existence of four distinct nuclear spin isomers of ethylene, which are characterized by different symmetries of nuclear and rotational wavefunctions. As a consequence, the four nuclear spin isomers of ethylene have different sets of allowed rotational energy levels and different absorption lines in the vibrational-rotational spectrum.

2.2. Nuclear wavefunctions of ethylene spin isomers

Initially, sixteen nuclear spin wavefunctions of ethylene can be written in the Zeeman basis. The nuclear spin Hamiltonian for ethylene molecule is as follows:

$$H = -\omega I_z + 2\pi \sum_{i<j} J_{ij}(I_i \cdot I_j),$$

where I_i, I_j – nuclear spin operators for spins *i* and *j,* respectively ($i, j = 1, \ldots, 4$); J_{ij} – *J*-coupling constant between spins *i* and *j*; I_z– projection onto the z-axis of the nuclear angular momentum operator; ω – angular precession frequency.

In order to find nuclear spin eigenfunctions of ethylene, it is necessary to carry out symmetrization operation in the D_{2h} group by diagonalizing the nuclear spin Hamiltonian using the molecular reference frame shown in Fig. S1:

$$I = 2 \in A_g^q: \begin{cases} \varphi_1 = |\alpha\alpha\alpha\alpha\rangle \\ \varphi_2 = \frac{|\alpha\alpha\alpha\beta\rangle}{2} + \frac{|\alpha\alpha\beta\alpha\rangle}{2} + \frac{|\alpha\beta\alpha\alpha\rangle}{2} + \frac{|\beta\alpha\alpha\alpha\rangle}{2} \\ \varphi_3 = \frac{|\alpha\alpha\beta\beta\rangle}{\sqrt{6}} + \frac{|\alpha\beta\alpha\beta\rangle}{\sqrt{6}} + \frac{|\alpha\beta\beta\alpha\rangle}{\sqrt{6}} + \frac{|\beta\alpha\alpha\beta\rangle}{\sqrt{6}} + \frac{|\beta\alpha\beta\alpha\rangle}{\sqrt{6}} + \frac{|\beta\beta\alpha\alpha\rangle}{\sqrt{6}}, \\ \varphi_4 = \frac{|\alpha\beta\beta\beta\rangle}{2} + \frac{|\beta\alpha\beta\beta\rangle}{2} + \frac{|\beta\beta\alpha\beta\rangle}{2} + \frac{|\beta\beta\beta\alpha\rangle}{2} \\ \varphi_5 = |\beta\beta\beta\beta\rangle \end{cases}$$

$$I = 1 \in B_{1u}^t: \begin{cases} \varphi_6 = \frac{|\beta\beta\beta\alpha\rangle}{2} + \frac{|\beta\beta\alpha\beta\rangle}{2} - \frac{|\beta\alpha\beta\beta\rangle}{2} - \frac{|\alpha\beta\beta\beta\rangle}{2} \\ \varphi_7 = -\frac{|\beta\beta\alpha\alpha\rangle}{\sqrt{2}} + \frac{|\alpha\alpha\beta\beta\rangle}{\sqrt{2}} \\ \varphi_8 = -\frac{|\alpha\alpha\alpha\beta\rangle}{2} - \frac{|\alpha\alpha\beta\alpha\rangle}{2} + \frac{|\alpha\beta\alpha\alpha\rangle}{2} + \frac{|\beta\alpha\alpha\alpha\rangle}{2} \end{cases},$$

$$I = 1 \in B_{2u}^t: \begin{cases} \varphi_9 = -\frac{|\beta\beta\beta\alpha\rangle}{2} + \frac{|\beta\beta\alpha\beta\rangle}{2} - \frac{|\beta\alpha\beta\beta\rangle}{2} + \frac{|\alpha\beta\beta\beta\rangle}{2} \\ \varphi_{10} = -\frac{|\beta\alpha\beta\alpha\rangle}{\sqrt{2}} + \frac{|\alpha\beta\alpha\beta\rangle}{\sqrt{2}} \\ \varphi_{11} = \frac{|\alpha\alpha\alpha\beta\rangle}{2} - \frac{|\alpha\alpha\beta\alpha\rangle}{2} + \frac{|\alpha\beta\alpha\alpha\rangle}{2} - \frac{|\beta\alpha\alpha\alpha\rangle}{2} \end{cases},$$

$$I = 1 \in B_{3g}^t: \begin{cases} \varphi_{12} = -\frac{|\beta\beta\beta\alpha\rangle}{2} + \frac{|\beta\beta\alpha\beta\rangle}{2} + \frac{|\beta\alpha\beta\beta\rangle}{2} - \frac{|\alpha\beta\beta\beta\rangle}{2} \\ \varphi_{13} = -\frac{|\alpha\beta\beta\alpha\rangle}{\sqrt{2}} + \frac{|\beta\alpha\alpha\beta\rangle}{\sqrt{2}} \\ \varphi_{14} = -\frac{|\alpha\alpha\alpha\beta\rangle}{2} + \frac{|\alpha\alpha\beta\alpha\rangle}{2} + \frac{|\alpha\beta\alpha\alpha\rangle}{2} - \frac{|\beta\alpha\alpha\alpha\rangle}{2} \end{cases},$$

$$I = 0 \in A_g^{Sa}: \left\{\varphi_{15} = \frac{1}{2\sqrt{1-\mu+\mu^2}}(-\mu\,|\beta\beta\alpha\alpha\rangle + |\beta\alpha\beta\alpha\rangle + (\mu-1)|\beta\alpha\alpha\beta\rangle + (\mu-1)|\alpha\beta\beta\alpha\rangle + |\alpha\beta\alpha\beta\rangle - \mu|\alpha\alpha\beta\beta\rangle),\right.$$

$$I = 0 \in A_g^{Sb}: \left\{\varphi_{16} = \frac{1}{2\sqrt{3(1-\mu+\mu^2)}}((\mu-2)\,|\beta\beta\alpha\alpha\rangle - (2\mu-1)|\beta\alpha\beta\alpha\rangle + (\mu+1)|\beta\alpha\alpha\beta\rangle + (\mu+1)|\alpha\beta\beta\alpha\rangle\right.$$
$$\left.- (2\mu-1)|\alpha\beta\alpha\beta\rangle + (\mu-2)|\alpha\alpha\beta\beta\rangle),\right.$$

$$\mu = \frac{\sqrt{J_g^2 + J_c^2 + J_t^2 - (J_g * J_c + J_g * J_t + J_t * J_c)} - (J_c - J_g)}{J_g - J_t},$$

where J_g, J_c, and J_t are *J*-couplings in ethylene for geminal, *cis*-, and *trans*-protons, respectively (see Section 3.1 of this SI).

Additional Results

3.1. The proton-proton *J*-coupling in studied molecules

The *J*-couplings for ethylene were taken from the literature.[10] The literature *J*-coupling values for 2-bromoethanol[11] were used as a starting point and then were adjusted until the simulated spectra fit the data. BrEtOD is an AA'BB' or an AA'XX' system depending on the field strength of an NMR spectrometer used. The appearance of its NMR spectrum is defined by the two geminal J_{gem} and the two vicinal J_{vic} proton-proton coupling constants. In this case of AA'BB' NMR spectra, it is convenient to use the symmetric coupling parameters defined and provided in Table S1.

Table S1. The symmetric coupling parameters for BrEtOD taken from the literature and their adjusted values.

Symmetric coupling parameters	From Ref.[11], Hz	Experimental, Hz
$K = J_{gem}(CH_2OD) + J_{gem}(CH_2Br)$	-22.55	-23.4
$M = J_{gem}(CH_2Br) - J_{gem}(CH_2OD)$	1.85	1.8
$N = J_{vic} + J'_{vic}$	11.50	10.4
$L = \lvert J_{vic1} - J'_{vic} \rvert$	1.40	2.4

The K constant defines the position of the low-intensity satellite signals in ^{1}H NMR PASADENA spectra of hyperpolarized BrEtOD; thus, the K value of -23.4 Hz was found. The M, N, and L constants were found from ^{1}H NMR spectra in thermal equilibrium acquired at 1.4 T (Fig. S2). The geminal *J*-couplings in BrEtOD were determined as -12.6 and -10.8 Hz. In order to decide which value belongs to the CH_2Br group and which to the CH_2OD group, data reported by Bernstein and Sheppard was used.[12] They reported values for the geminal coupling constants of 10.2±0.2 and 10.8±0.4 Hz for CH_2DBr and CH_2DOH, respectively. Using this data, the -10.8 Hz coupling is assigned to the geminal hydrogens adjacent to the bromine and the -12.65 Hz value to the hydroxyl methylene group. The values of J_{vic} and J_{vic}' are determined largely by the conformational properties of the X-CH_2-CH_2-Y fragment and present rotationally averaged constants.

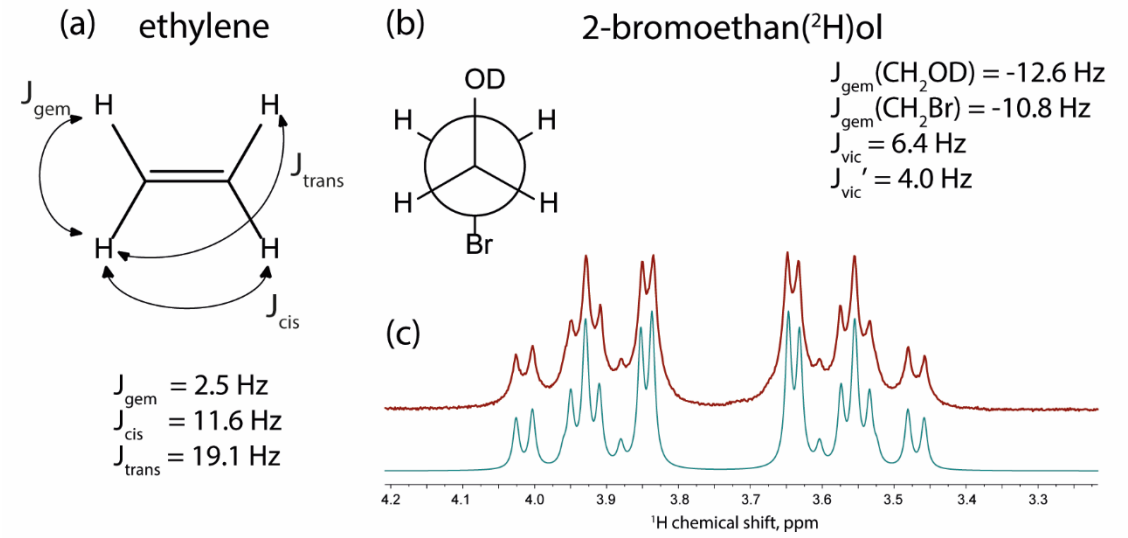

Figure S2. The *J*-couplings for ethylene (a) and 2-bromoethan(^{2}H)ol (b) used in this work. (c) The experimental (red) ^{1}H NMR spectrum of 2-bromoethanol acquired at 1.4 T NMR benchtop spectrometer and the corresponding simulated spectrum (teal).

3.2. The optimization of OPSY pulse sequence

In order to filter out thermal NMR signals and obtain only the spectrum resulting from the $I_{zi} \cdot I_{zj}$ terms (*i*,*j* – corresponding protons of BrEtOD inherited from the p-H_2 molecule), we used OPSY-d12 pulse sequence.[7] The graphical representation of the pulse sequence is given below:

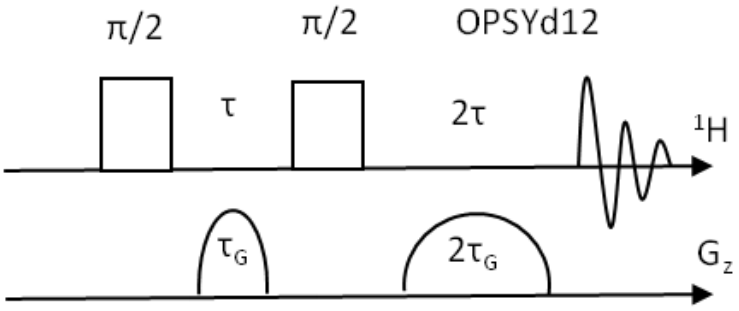

Figure S3. The schematic representation of OPSYd-12 pulse sequence used in this work.

In the case of OPSYd-12 the parameter which defines the spectrum intensity is τ. Variation of τ has shown that $\tau=\tau_G$=1 ms provides a spectrum with close to the theoretical maximum intensity (50% of intensity obtained in a single π/4 pulse experiment), therefore it was used in the experiments.

3.3. ^{1}H NMR spectra analysis

All spectra were simulated in MATLAB. The script is provided in *Appendix A*. In brief, the initial spin density matrices for ethylene were constructed in the basis of Zeeman functions using the populations of the corresponding Hamiltonian eigenstates obtained previously for ethylene.[13] Due to symmetry constraints imposed on nuclear relaxation in ethylene we described the initial spin density matrix of ethylene in terms of the populations of the corresponding irreducible representations (A_g, B_{3g}, B_{1u}, and B_{2u}).

OPSYd-12 spectra of BrEtOD at different storage times of ethylene in a syringe

As was shown previously, *syn*-addition of p-H_2 to acetylene (*Z*-ethylene) results in population of the two singlet eigenstates $A_g^{S_a}$ and $A_g^{S_b}$ as well as the states belonging to B_{1u} and B_{3g}, while *anti*-addition of p-H_2 (*E*-ethylene) leads to the population of $A_g^{S_a}$, $A_g^{S_b}$, B_{1u}, and B_{2u}.[13] It should be noted that the initial spin density matrix constructed for ethylene includes only the populations of the corresponding eigenstates, because the coherences are expected to be averaged out over the distribution of product formation times. The same averaging is also applied to the spin density matrix of BrEtOD inherited from the p-H_2-labelled ethylene, and is a common approach for the description of parahydrogen-induced hyperpolarization (PHIP) spectra.[14] Interconversion of nuclear spin isomers was introduced in the A_g subensemble with a short characteristic time ≤1 s, because all the ^{1}H NMR spectra of BrEtOD obtained at the minimum ethylene travel time (1 s) resemble those of ethylene with an equilibrated A_g subensemble. Interconversion of nuclear spin isomers within the *g* ($B_{3g} \rightleftarrows A_g$) manifold and the *u* manifold ($B_{1u} \rightleftarrows B_{2u}$) and between the *g* and *u* manifolds was introduced with characteristic times close to those obtained by fitting the OPSY signal decay (see Fig. 3 in the main text) and reported earlier.[13] In the general case, the rates of interconversion within the g and u manifolds can be different, however we couldn't observe this difference in the OPSY signal decay kinetics, as it was fitted well by mono- (imbalance between the g and u manifolds is absent) or biexponential function (imbalance between the g and u manifolds is present), so for simulation purpose the rates of interconversion within the g and u manifolds were taken to be equal. The detection step included a π/4 rf pulse followed by the FID acquisition using the spin Hamiltonian for BrEtOD. We used a standard π/4 pulse scheme for simulation of OPSY-d12 spectra because at $\tau<<\frac{1}{2\cdot\pi\cdot J}$ (where *J* is the vicinal coupling constant of the p-H_2-derived protons in BrEtOD) both the π/4 single-pulse sequence and OPSY-d12 provide antiphase terms proportional to $I_{iz}\cdot I_{j-} + I_{i-}\cdot I_{jz}$.[7]

The simulation of the experimental OPSY spectrum of BrEtOD with a single 45° pulse model calculations seems justified since ^{1}H NMR spectra for both pulse sequences (45° single pulse and OPSY) are by far dominated by the 2-spin order in our study. To verify this, we analyzed the dependence of the NMR signal intensity after a single rf pulse on the pulse flip angle. The Fourier transformation of such dependence provides a spectrum with several different harmonics (sin(nϕ), Figure S4), each of which can contain contributions from one or more different spin orders[15]. To evaluate the relative contributions of different spin orders separately, we performed simulations for different initial spin states of ethylene, namely those corresponding to Z-ethylene (Figure S4a) as well as the 3-spin (Figure S4b) and 4-spin order (Figure S4c). Trace c was normalized such that the sin(4ϕ) peaks in both a and c have the same amplitude because both peaks originate from 4-spin order only. A similar normalization was used for trace b.

Figure S4 clearly demonstrates that the contribution of the 2-spin order is more than an order of magnitude larger than the contribution of other spin orders: the contributions of 3- and 4-spin orders are totally negligible. This is not surprising, as parahydrogen is characterized by the 2-spin order, which is transferred to the hydrogenation products and thus constitutes the dominating contribution. The sin(ϕ) component, which corresponds to an in-

phase NMR signal, is always present to the extent that the spin system of a product deviates from the weak coupling regime. Compared to Figure S4, its relative contribution to the spectra is further reduced because the 45° flip angle maximizes the contribution of the sin(2ϕ) component (antiphase NMR signal) but partially suppresses that of the sin(ϕ) component. Higher orders (3 and 4) are clearly not generated to any significant extent.

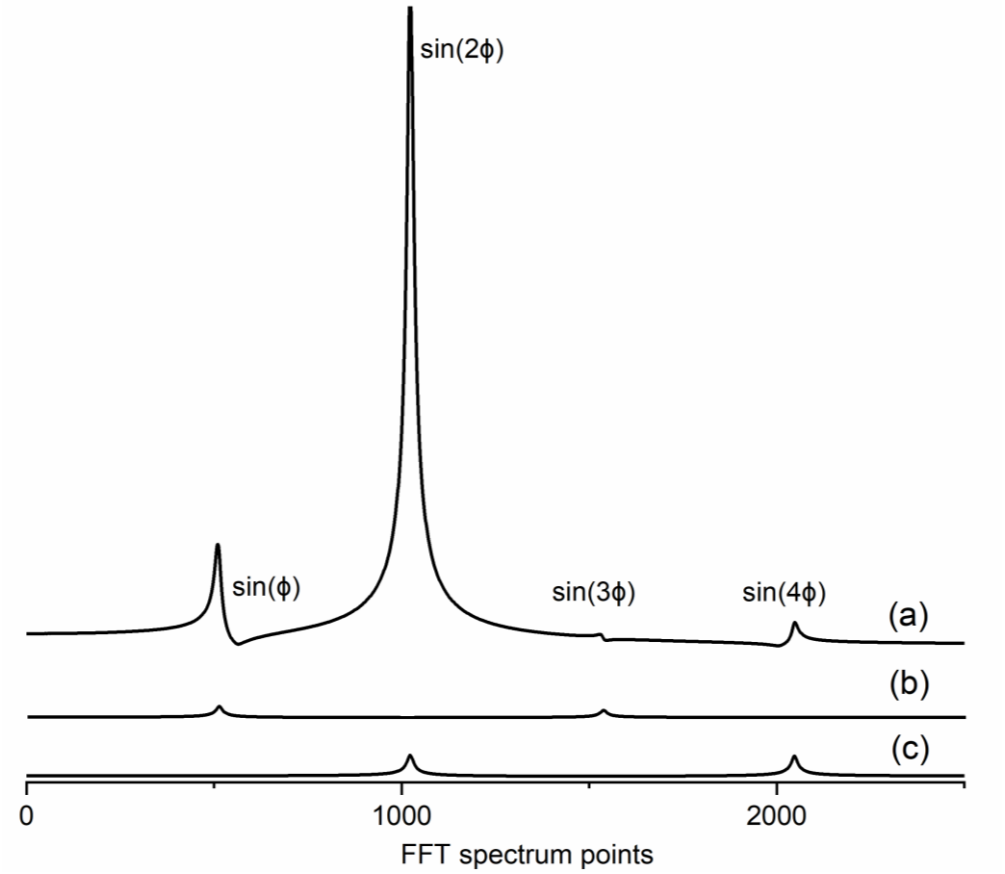

Figure S4. Fourier transform of the dependence of the calculated intensity of the ^{1}H NMR spectrum of BrEtOD produced by a single rf pulse on the pulse flip angle (ϕ). a) The initial spin state corresponds to Z-ethylene obtained using Ir-P@SiO_2 catalyst. b) The initial spin state corresponds to the spin density matrix constructed as a sum of 3-spin orders of the four protons of ethylene. c) The initial spin state corresponds to the spin density matrix constructed as 4-spin order of the four protons of ethylene.

The experimental and simulated spectra at different storage times of ethylene in the syringe obtained for different catalysts are presented in Figures S5-S7. The variable parameter was the relative fraction of E-ethylene (χ(E) = 1- χ(Z)). Overall, the simulated and experimental spectra demonstrate good agreement, though some discrepancies are present, which may be related to the fact that the nuclear relaxation in BrEtOD is not considered.

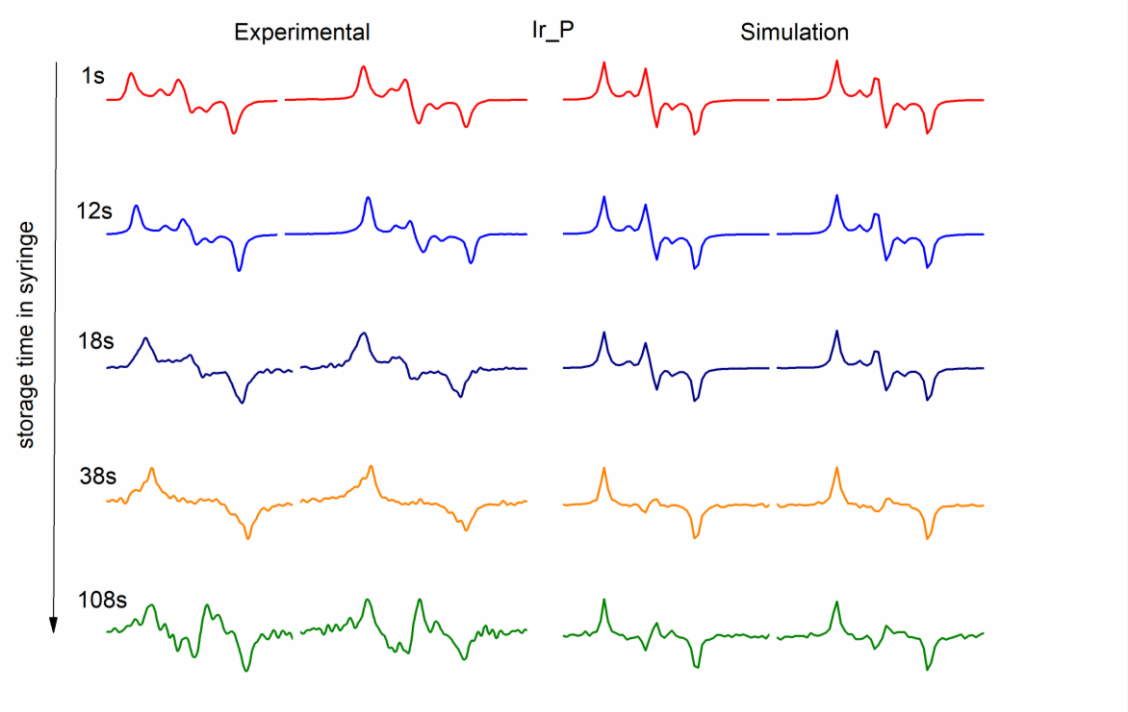

Figure S5. Experimental and simulated OPSY spectra of BrEtOD obtained at different ethylene storage times in the syringe. Ir-P@SiO_2 was used for ethylene production via heterogeneous hydrogenation of acetylene with p-H_2. The fraction of *E*-ethylene was found to be ~0.3%.

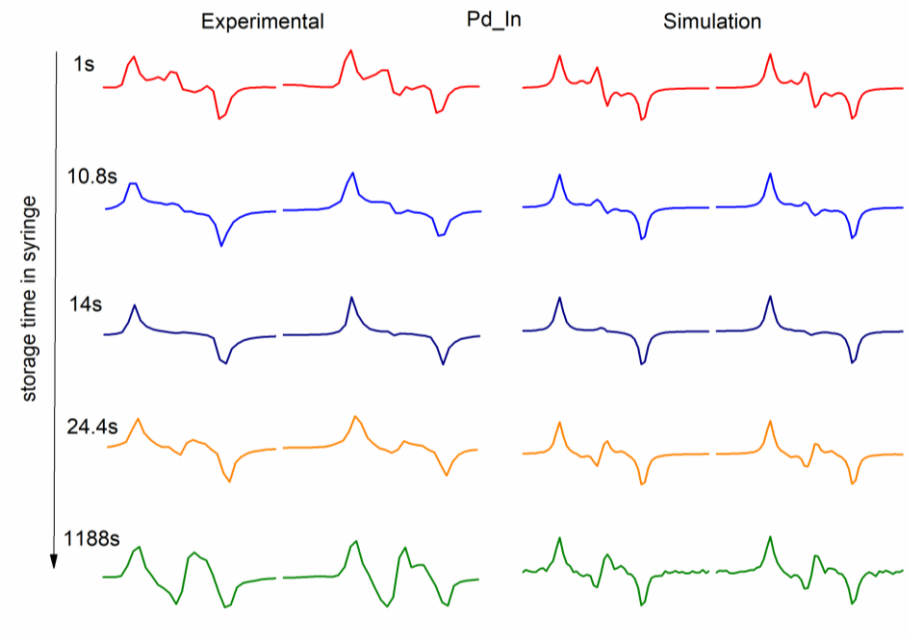

Figure S6. Experimental and simulated OPSY spectra of BrEtOD obtained at different ethylene storage times in the syringe. Pd-In/Al_2O_3 was used as a catalyst for ethylene production. The fraction of *E*-ethylene was found to be ~8%.

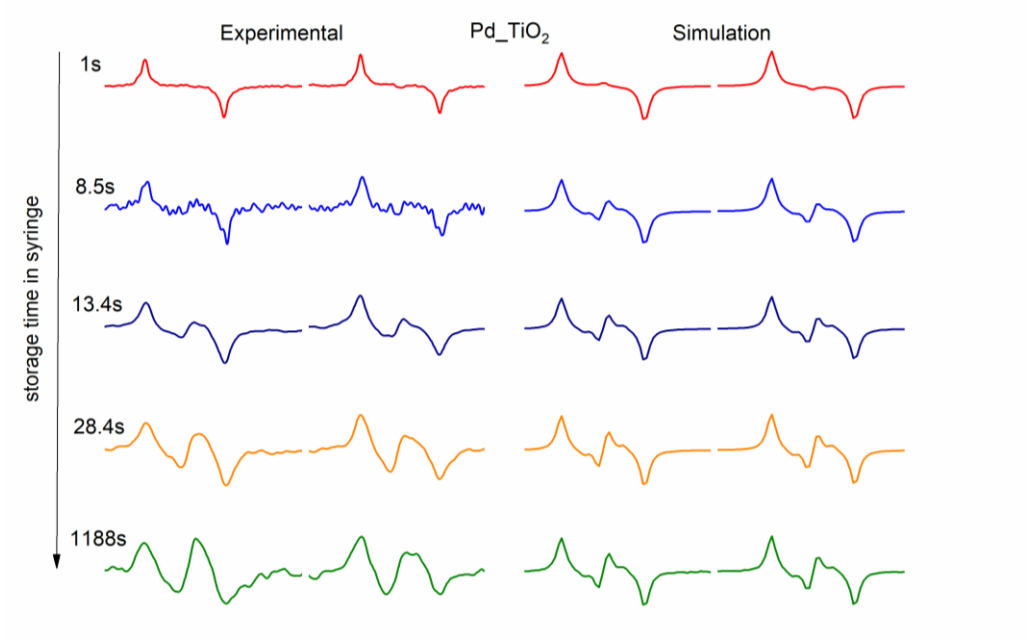

Figure S7. Experimental and simulated OPSY spectra of BrEtOD obtained at different ethylene storage times in the syringe. Pd/TiO_2 was used as a catalyst for ethylene production. The fraction of *E*-ethylene was found to be ~45%.

Studying the activation of Ir-P@SiO_2 catalyst

The signal enhancement achieved over immobilized Ir-P@SiO_2 is a more sensitive indicator of catalyst activation than catalytic conversion: note that the *SE* values go up from 30±10 to the 200±80 in 40 min (Fig. S8).

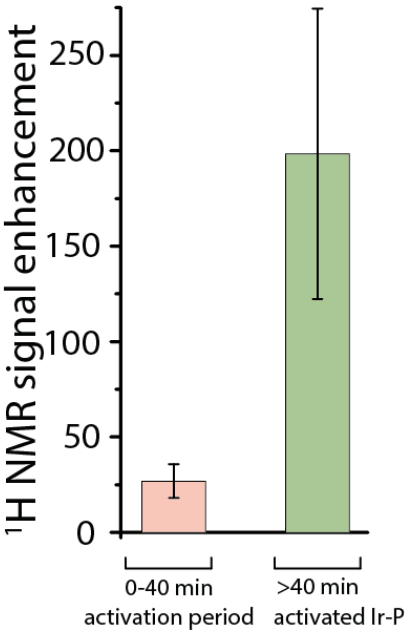

Figure S8. The observed ^{1}H NMR signal enhancement values for BrEtOD in the case of Ir-P@SiO_2 catalyst.

3.4. Calculations

Calculation of conversion in acetylene hydrogenation

The acetylene conversion value (*X*) at a certain flow rate and temperature was calculated as the molar ratio of the reaction products (ethylene and ethane) to the sum of products and unreacted acetylene. The selectivity to ethylene ($S_{ethylene}$) was calculated as the molar ratio of ethylene to the sum of the products. Both values were evaluated from ^{1}H NMR spectra acquired in thermal equilibrium after a complete relaxation of hyperpolarization.

Kinetics data processing

Each point on the graphs reflects the individual experiment. The x-axis error bars come from the uncertainty of time measurement using a digital timer, and the relative standard deviation (RSD) was set as 1 s. The error associated with OPSY signal integration depends on the signal-to-noise ratio (SNR) of the NMR signal. The SNR for CH_2OD-group signal in ^{1}H NMR spectra was determined. The RSD value for signal integral was calculated as $RSD = \frac{86}{SNR}$.[16] The y-axis error is calculated using two RSD values obtained for both integrals (in control spectrum and in experimental spectrum) assuming normal distribution of errors.

As mentioned in the main text, the correct kinetics data processing is vital for retrieving adequate model parameters. Here in this work, partial equilibration of ethylene NSIMs during the syringe filling was taken into account, in contrast to the previous work[13], in which zero ethylene storage time corresponds to the end of the syringe filling with ethylene. We propose the following algorithm: we take the OPSY spectrum recorded immediately after an abrupt interruption of ethylene bubbling into the NMR tube filled with bromine water as the first point on the graph. In this case, the equilibration process takes place only during the time-of-flight of the gas mixture along the gas lines. Based on the geometry of the setup, the ethylene time-of-flight from the syringe (or the reactor) to the NMR tube was estimated as 1 s (see below). Therefore, for the first kinetic point, we use $T_{storage}$ = 1 s.

Additionally, for experiments with Ir-P@SiO_2 catalyst, the initial points with short storage times were obtained by increasing the gas lines volume with the flow rates being unchanged. This was achieved by inserting a piece of a 6.3 mm. o.d. PTFE tubing in the gas line. This way the delivery time of ethylene from the reactor was increased from 1 s to 6 or 12 s, depending on the length of the added segment.

We normalized each experimental point to the so-called control point. For the control experiment the spectrum was recorded immediately after bubbling a mixture of products through bromine water without syringe filling. The control experiment was introduced in order to minimize the effect of perturbations in the setup: reactor temperatures and related minor changes in catalyst conversion; bromine concentration deviations. The difference in moles of the products that enter the NMR tube in control and the experiment with the syringe was taken into account. Knowing conversion value, the volume of supply lines (3.4 mL for standard case; 15.9 mL and 31.8 are additional volumes of added segments used in experiment with Ir-P@SiO_2 catalyst), and the time of bubbling gives the information about the moles of ethylene entering the NMR tube in each experiment. Moreover, the decrease of the flow rate

after the reactor is also taken into account. This happens since the overall number of moles is decreased during the hydrogenation (A+B→C). The volumetric flow rate was recalculated according to the formula presented below.

Storage time calculations

In order to correctly analyze the equilibration kinetics of ethylene NSIMs, it is necessary to understand what is the effective time that ethylene molecules are stored during the syringe filling.

Let's suppose that ethylene molecules are drawn into the syringe with a constant rate over time (T). Some ethylene molecules will be stored in the syringe for 0 seconds (those that entered the syringe at the last moment), and some of them – for T seconds (those that entered the syringe at the first moment). We also assume that the gas in the syringe is ideally mixed and ethylene is equilibrating monoexponentially with the time constant T_{short} according to the following equation:

$$A = A_0 e^{-\frac{t}{T_{short}}}.$$

Then the average value of the "polarized" signal of an ensemble of ethylene molecules ($\overline{A}$) can be found as a definite integral of the value of the ethylene signal (A_0) normalized by the time it takes to fill the syringe:

$$\overline{A} = \frac{\int_0^T A_0 \, e^{-\frac{t}{T_{short}}} dt}{T} = \frac{A_0 \cdot T_{short}}{T}\left(1 - e^{-\frac{T}{T_{short}}}\right).$$

Based on the ergodic hypothesis, we can assume that averaging over time is equivalent to averaging over the ensemble. Then:

$$\overline{A} = A_0 e^{-\frac{\overline{t}}{T_{short}}} = \frac{A_0 \cdot T_{short}}{T}\left(1 - e^{-\frac{T}{T_{short}}}\right).$$

Therefore, the effective time that ethylene molecules are stored during the syringe filling can be described as:

$$\overline{t} = -T_{short} \ln\left(\frac{T_{short}}{T}\left(1 - e^{-\frac{T}{T_{short}}}\right)\right).$$

For example, if T_{short}=6 s and T=20 s, the average storage time ($\overline{t}$) is 7.4 s. If T_{short}=10 s and T=20 s, the average storage time ($\overline{t}$) is 8.4 s. The time of syringe filling was varied from 5 to 20 s, depending on the experiment. For such values, the assumption of a monoexponential decay is valid with high accuracy, since $T_{long} \sim 10^3$ s in biexponential fit.

The total storage time (t_{total}) of ethylene in the syringe was calculated as the sum of the average time that ethylene molecules are stored during the syringe filling ($\overline{t}$) and the storage time of ethylene in the syringe $t_{storage}$:

$$t_{total} = \overline{t} + t_{storage}.$$

Time-of-flight calculations

It can be assumed that the reaction proceeds in an ideal plug-flow reactor. Because the number of molecules in the gas phase decreases during the hydrogenation, the gas flow rate also decreases along the reactor and depends on the total conversion of acetylene (*X*) and selectivity to ethylene ($S_{ethylene}$). The gas flow rate (U) after the reactor can be found using the following equation (the molar ratio of acetylene : p-H_2 is 1 : 4):

$$U = U_0 \cdot \frac{5 - (2 - S) \cdot X}{5},$$

where U_0 is the supply rate of acetylene : pH_2 mixture to the reactor. The time-of-flight was calculated as the ratio of the total volume of gas supply lines (from the reactor to NMR tube) to the reactor outflow rate.

T_1 measurements

The longitudinal relaxation time (T_1) of protons in ethylene in the gas phase was measured using the standard inversion-recovery pulse sequence. It was found that T_1 for ethylene protons is 250±15 ms under experimental conditions (atmospheric pressure, room temperature, ethylene : H_2 mixture in the molar ratio of 1 : 3).

References

[1] O. G. Salnikov, D. B. Burueva, L. M. Kovtunova, V. I. Bukhtiyarov, K. V. Kovtunov, I. V. Koptyug, *ChemPhysChem* **2022**, *23*, e202200072.

[2] I. V. Skovpin, S. V. Sviyazov, D. B. Burueva, L. M. Kovtunova, A. V. Nartova, R. I. Kvon, V. I. Bukhtiyarov, I. V. Koptyug, *Dokl. Phys. Chem.* **2023**, *512*, 149–157.

[3] I. V. Skovpin, L. M. Kovtunova, A. V. Nartova, R. I. Kvon, V. I. Bukhtiyarov, I. V. Koptyug, *Catal. Sci. Technol.* **2022**, *12*, 3247–3253.

[4] D. B. Burueva, A. Y. Stakheev, I. V. Koptyug, *Magn. Reson.* **2021**, *2*, 93–103.

[5] I. S. Mashkovsky, N. S. Smirnova, P. V. Markov, G. N. Baeva, G. O. Bragina, A. V. Bukhtiyarov, I. P. Prosvirin, A. Y. Stakheev, *Mendeleev Commun.* **2018**, *28*, 603–605.

[6] D. B. Burueva, K. V. Kovtunov, A. V. Bukhtiyarov, D. A. Barskiy, I. P. Prosvirin, I. S. Mashkovsky, G. N. Baeva, V. I. Bukhtiyarov, A. Y. Stakheev, I. V. Koptyug, *Chem. - Eur. J.* **2018**, *24*, 2547–2553.

[7] A. N. Pravdivtsev, V. P. Kozinenko, J.-B. Hövener, *J. Phys. Chem. A* **2018**, *122*, 8948–8956.

[8] L. D. Landau, E. M. Lifshitz, *Quantum Mechanics. Non-Relativistic Theory*, Elsevier, **1977**.

[9] P. L. Chapovsky, V. V. Zhivonitko, I. V. Koptyug, *J. Phys. Chem. A* **2013**, *117*, 9673–9683.

[10] R. M. Lynden-Bell, N. Sheppard, *Proc. R. Soc. London. Ser. A. Math. Phys. Sci.* **1962**, *269*, 385–403.

[11] R. C. Hirst, D. M. Grant, *J. Chem. Phys.* **1964**, *40*, 1909–1918.

[12] H. J. Bernstein, N. Sheppard, *J. Chem. Phys.* **1962**, *37*, 3012.

[13] V. V. Zhivonitko, K. V. Kovtunov, P. L. Chapovsky, I. V. Koptyug, *Angew. Chem. Int. Ed.* **2013**, *52*, 13251–13255.

[14] C. R. Bowers, in *Encycl. Magn. Reson.* (Eds.: R.K. Harris, R. Wasylishen), John Wiley, Chichester, UK, **2007**, pp. 750–770.

[15] E. A. Nasibulov, A. N. Pravdivtsev, A. V. Yurkovskaya, N. N. Lukzen, H.-M. Vieth, K. L. Ivanov, *Zeitschrift für Phys. Chemie* **2013**, *227*, 929–953.

[16] P. A. Hays, T. Schoenberger, *Anal. Bioanal. Chem.* **2014**, *406*, 7397–7400.

Appendix A. Matlab script

```
function ethylene_NSI()
% Definition of single spin operators and their sums for N-spin system %
unit=[1,0;0,1]; sigma_x=1/2*[0,1;1,0]; sigma_y=1/2*[0,1i;-1i,0]; sigma_z=1/2*[1,0;0,-1];
sigma = {sigma_x,sigma_y,sigma_z};
I = {}; E=unit;
nspins=4;
for i = 1:nspins
for k = 1:length(sigma)
I{i,k} = sigma{k};
for a = 1:i-1
I{i,k} = kron(unit,I{i,k});
end
for b = 1:nspins-i
I{i,k} = kron(I{i,k},unit);
end
end
end
for i = 1:nspins-1
E = kron(E,unit);
end
I_sum = {};
for k = 1:length(sigma)
I_sum{k} = zeros(2^nspins);
for i = 1:nspins
I_sum{k} = I_sum{k} + I{i,k};
end
end
V = {};
for i = 1:2^nspins
V{i} = zeros(2^nspins,1);
end
%% Ethylene eigenstates %%
% V1-V16 - basis eigenfunctions of ethylene nuclear spin hamiltonian %
V{1}(16)=1; V{5}(1)=1;
for i=[8,12,14,15]
V{2}(i)=0.5;
end
for i=[4,6,7,10,11,13]
V{3}(i)=1/sqrt(6);
end
for i=[2,3,5,9]
V{4}(i)=0.5;
end
for i=[14,15]
for k=[8,12]
V{6}(k)=-0.5;
end
V{6}(i)=0.5;
end
V{7}(4)=1/sqrt(2);
V{7}(13)=-1/sqrt(2);
for i=[9,5]
for k=[3,2]
V{8}(k)=-0.5;
end
V{8}(i)=0.5;
end
for i=[14,8]
for k=[15,12]
V{9}(k)=-0.5;
end
V{9}(i)=0.5;
end
V{10}(6)=1/sqrt(2);
V{10}(11)=-1/sqrt(2);
for i=[5,2]
for k=[9,3]
V{11}(k)=-0.5;
end
V{11}(i)=0.5;
end
for i=[12,14]
for k=[15,8]
V{12}(k)=-0.5;
end
V{12}(i)=0.5;
end
V{13}(10)=1/sqrt(2);
V{13}(7)=-1/sqrt(2);
for i=[5,3]
for k=[9,2]
V{14}(k)=-0.5;
end
V{14}(i)=0.5;
end
% V15 %
V{15}(13)=0.267; V{15}(11)=1; V{15}(10)=-1.267; V{15}(7)=-1.267; V{15}(6)=1; V{15}(4)=0.267; V{15}=V{15}./2.31;
% V16 %
V{16}(13)=-2.267; V{16}(11)=1.534; V{16}(10)=0.733; V{16}(7)=0.733; V{16}(6)=1.534; V{16}(4)=-2.267; V{16}=V{16}./4;
% Population of eigenstates rho{1..16} %
rho = {};
for i = 1:2^nspins
rho{i} = V{i}*V{i}';
end
% Population of the ethylene irreducible representations %
% Ag population %
rho_Ag = zeros(16);
```

```
for i=1:5
rho_Ag = rho_Ag+rho{i};
end
for k=15:16
rho_Ag = rho_Ag+rho{k};
end
% B3g population %
rho_B3g = zeros(16);
for i=12:14
rho_B3g = rho_B3g+rho{i};
end
% B1u population %
rho_B1u = zeros(16);
for i=6:8
rho_B1u = rho_B1u+rho{i};
end
% B2u population %
rho_B2u = zeros(16);
for i=9:11
rho_B2u = rho_B2u+rho{i};
end
% Population of Z ethylene eigenstates %
rho_Ag_cis=0.12*rho{15}+0.13*rho{16};
rho_B3g_cis=0.125*rho_B3g;
rho_B1u_cis=0.125*rho_B1u;
rho_cis=rho_B3g_cis + rho_B1u_cis + rho_Ag_cis;
% Population of E ethylene eigenstates %
rho_Ag_trans=0.02*rho{15}+0.23*rho{16};
rho_B1u_trans=0.125*rho_B1u;
rho_B2u_trans=0.125*rho_B2u;
rho_trans=rho_B1u_trans+rho_B2u_trans+rho_Ag_trans;
% Averaged populations of the corresponding irreducible representations %
rho_Agav=0.25/7*rho_Ag;
rho_cis_Gav=(rho_Ag+rho_B3g)*(0.25+0.125*3)/10;
rho_trans_Gav=(rho_Ag+rho_B3g)*(0.25)/10;
rho_cis_Uav = (rho_B1u+rho_B2u)*(0.125*3)/6;
rho_trans_Uav = (rho_B1u+rho_B2u)*(0.125*6)/6;
% Totally averaged density matrix after full relaxation between G and U %
rho_averaged = 1/16*E;
%% Nuclear relaxation in ethylene %%
relaxation_time = 1188;
% R0 - matrix corresponding to relaxation in Ag subensemble %
damp_rate0=3;
R0=zeros(16);
R0=R0-E.*damp_rate0;
% R1- matrix corresponding to relaxation in G subensemble %
damp_rate=0.09;
R1=zeros(16);
R1=R1-E.*damp_rate;
% R2- matrix corresponding to relaxation in U subensemble %
damp_rate1=0.09;
R2=zeros(16);
R2=R2-E.*damp_rate1;
% R3- matrix corresponding to relaxation between U and G subensembles %
damp_rate2=0.001;
R3=zeros(16);
R3=R3-E.*damp_rate2;
% Relaxation superoperator %
function Rel = Rel(R)
Rel=expm(R*relaxation_time);
end
%% Nuclear relaxation in ethylene during syringe hold time (relaxation_time) %%
% x_Z/x_E - fraction of Z/E ethyelene %
x_Z = 0.92; x_E = 0.08;
rho_Agav_cis = Rel(R0)*(rho_Ag_cis-rho_Agav)*(Rel(R0))' + rho_Agav; rho_Agav_trans = Rel(R0)*(rho_Ag_trans-rho_Agav)*(Rel(R0))' + rho_Agav;
rho_cis_G_U_av = Rel(R1)*(rho_Agav_cis+rho_B3g_cis-rho_cis_Gav)*(Rel(R1))' + rho_cis_Gav + Rel(R2)*(rho_B1u_cis-rho_cis_Uav)*(Rel(R2))' + rho_cis_Uav;
rho_trans_G_U_av = Rel(R1)*(rho_Agav_trans-rho_trans_Gav)*(Rel(R1))' + rho_trans_Gav + Rel(R2)*(rho_B1u_trans+rho_B2u_trans-rho_trans_Uav)*(Rel(R2))' + rho_trans_Uav;
rho = Rel(R3)*(x_Z*rho_cis_G_U_av + x_E*rho_trans_G_U_av-rho_averaged)*(Rel(R3))' + rho_averaged;
%% 1H NMR of BrEtOH %%
% Zeeman frequency offsets and J coupling constants %
w0=2*pi*1230;
w1=2*pi*1038;
w2=2*pi*1146;
J12=-pi*12.6; J34=-pi*10.8;
J13=pi*6.4; J14=pi*4;
% Hamiltonian for BrEtOH %
H = (w0-w2)*(I{1,3}+I{2,3})+(w0-
w1)*(I{3,3}+I{4,3})+J12*(I{1,1}*I{2,1}+I{1,2}*I{2,2}+I{1,3}*I{2,3})+J34*(I{3,1}*I{4,1}+I{3,2}*I{4,2}+I{3,3}*I{4,3})+J13*(I{1,1}*I{3,1}+I{1,2}*I{3,2}+I{1,3}*I{3,3}+I{2,1}*I{4,1}+I{2,2}*I{4,2}+I{2,3}*I{4,3})+J14*(I{1,1}*
I{4,1}+I{1,2}*I{4,2}+I{1,3}*I{4,3}+I{2,1}*I{3,1}+I{2,2}*I{3,2}+I{2,3}*I{3,3});
timestep=1/norm(H);
%Pulse propagator%
function P_y = P_y(phi)
P_y=expm(-1i*I_sum{2}*phi);
end
%Time_evolution propagator%
function Evol = Evol(steps)
Evol=expm(-1i*H*timestep*steps);
end
% Detection coil %
coil = (I_sum{1}+1i*I_sum{2});
%% Pulse sequence - P1 pulse - FID %%
% Averaging of coherences due to different times of reaction product (BrEtOH) formation %
D1=1;
rho_av_=0;
for i=0:(D1/timestep)
rho_av_=rho_av_+Evol((D1/timestep)-i)*rho/(D1/timestep)*(Evol((D1/timestep)-i))';
end
% P1 pulse (phase y) %
rho = P_y(-pi/4)*rho_av_*(P_y(-pi/4))';
```

```
% Acquisition %
fid = zeros(2048*8,1);
for i =1:2048*8
fid(i)=trace(coil'*rho);
rho = Evol(1)*rho*Evol(1)';
end
% Window function %
window_function = exp(-12*linspace(0,1,2048*8))';
fid=fid.*window_function;
% Noise %
noise = (randn(1,2048*8))/256;
% Fourie transform %
spectrum = fftshift(fft(fid))+noise';
% Plotting %
figure()
plot(real(spectrum));
xlim([1100*8,1300*8]);
end
```